https://ntrs.nasa.gov/search.jsp?R=19670009755 2018-07-24T11:03:29+00:00Z

CONTINUUM ELECTROMECHANICS GROUP

ELECTROMECHANICAL

STREAM-STRUCTURE INSTABILITIES

by Frederick D. Ketterer

NsG-368 CSR-TR-66-16 August 1966

ELECTROMECHANICAL STREAM-STRUCTURE INSTABILITIES

by

Frederick D. Ketterer

Department of Electrical Engineering
Massachusetts Institute of Technology
Cambridge, Massachusetts

ABSTRACT

The problem of a highly conducting fluid stream coupled by means of a transverse electric or parallel magnetic field to a conducting elastic medium is examined in detail. From the dispersion relation and the Bers-Briggs criterion the stability of the infinite length system is described. Eigenfrequencies and eigenfunctions are computed for the finite length system and good agreement is obtained with experiments performed with an electrohydrodynamic system. A physical explanation is given for the overstabilities observed. The close analogy between a limiting case of the field coupled system and an electron beam coupled to a traveling wave structure is discussed.

I Introduction

Stream structure interactions occur in many physical areas and have great practical significance. The flow of air over panels is known to cause wing flutter and instabilities in aircraft.[1,2]

Numerous electron beam devices, such as the traveling wave tube, klystron, backward wave amplifier and oscillator, among others, make use of the instabilities produced by the coupling of an electron beam to a passive structure.[3] Haus[4] has analyzed the problem where magneto acoustic waves in a moving plasma couple to a passive structure to produce wave amplification. The present system is the first, to the author's knowledge, which couples a fluid stream to a mechanical structure by means of an electric or magnetic field.

Perhaps the first experiment concerning a stream-structure interaction was performed by Lord Rayleigh,[5] who impressed the vibrations of a water jet, produced by capillary instability of the sausage mode, onto a sounding board and mechanically fed back the vibrations to the entrance of the flow, producing large oscillations of the jet.

The overstability is of course due to the regenerative feedback through the external mechanical linkage and strictly speaking the system is not of the stream-structure type in the context of this paper. Suppose however, the external feedback link is replaced by a structure* which can couple to the stream at each point along its length. Then if a wave on the stream traveling downstream can couple to a wave on the structure in such a way that some of the wave energy can be fed back to

* Structure in the context of this paper implies a mechanical structure capable of transverse vibrations such as a tuning fork, membrane, or in the case of the experiment to be described, a weak spring.

the upstream end, the conditions for self oscillation may exist with the system overstable. Under other conditions, the stream and structure may still couple to produce an amplifying wave, and under certain circumstances the structure may damp the wave.

The stream-structure system to be studied here is shown in Fig. 1 and consists of a conducting liquid jet and a conducting membrane coupled by an electric or magnetic field. The jet is considered to be thin and only the kink mode will be discussed. As the jet or membrane is displaced in the transverse direction, the field is perturbed, producing a net traction on the element perturbed (self coupling), and also producing a net traction on the other deformable element (mutual coupling). Mechanical tension and end effects are important.

While the behavior of many stream structure interactions is understood qualitatively, it is only recently that effort has been made to analytically compute the complex eigenfrequencies for a stream-structure device of finite length.(6) The stability of the infinitely long system will be examined from the dispersion relation and the Bers-Briggs(7,8) criterion, and the eigenfrequencies and eigenfunctions computed for the finite length system. It will be shown that the necessary ingredients for self oscillation (overstability) are present for both electric and magnetic field coupling, and that experiments performed on the electrohydrodynamic system exhibit overstability in quantitative agreement with theory.

II Problem Description

In a previous paper,(9) the author has considered the dynamics of two highly conducting finite length fluid streams coupled by an electric or magnetic field. It was shown that there were four basically different

classes of flow: Class I: subcapillary, Class II: supercapillary co-streaming, Class III: supercapillary counter-streaming, and Class IV: ~~Subcapillary~~ supercapillary flow. The first three classes were discussed in that paper; the Class IV flow will be the topic of the present paper.

The model for the system consists of a planar conducting fluid stream of density ρ_1 and surface tension T_1 and a conducting elastic membrane* with density ρ_2 and tension per unit width T_2, coupled by a transverse electric field E_o or longitudinal magnetic field H_o. The assumed planar geometry simplifies the mathematics and it has been shown (9) that such a model is valid for a circular jet if the electrical coupling coefficients are experimentally determined. As in the previous paper the discussion will be restricted to the kink mode (m = 1) of the jet. If V_o is the stream velocity and ξ_1 and ξ_2 the transverse displacements of the stream and membrane, the dynamical equations are given by

$$\left[\frac{\partial}{\partial} + V_o \frac{\partial}{\partial}\right]^2 \xi_1 - V_{t_1}^2 \frac{\partial^2}{\partial^2}\xi_1 - \eta \frac{\omega_{e_1}^2}{2}\xi_1 = -\frac{1}{2}\,\omega_{e_2}^2\,\xi_2$$

$$\frac{\partial^2}{\partial t^2}\xi_2 - V_{t_2}^2 \frac{\partial^2}{\partial^2}\xi_2 - \eta \frac{\omega_{e_2}^2}{2}\xi_2 = -\frac{1}{2}\,\omega_{e_1}^2\,\xi_1 \qquad (1)$$

where $V_{t_{1,2}} = \sqrt{\dfrac{2T_{1,2}}{\rho_{1,2}\Delta}}$ $\qquad \omega_{e_{1,2}} = \sqrt{\dfrac{2\epsilon_o E_o^2}{(2a-\Delta)\rho_{1,2}\Delta}}$

$\eta = \dfrac{b+a - 3\,\Delta/2}{b - a - \Delta/2}$ $\qquad \omega_{h_{1,2}} = \sqrt{\dfrac{2\mu_o H_o^2}{(2a-\Delta)\rho_{1,2}\Delta}}$

The equations for magnetic coupling are obtained from Eq. (1) by

* The kink mode (m = 1) of a stationary fluid stream can be modeled by an elastic membrane.

replacing ω_e^2 by $-\omega_h^2$.

The assumptions used in the derivation and explanation of the quantities and terms in Eq. (1) are given in (9) and will be omitted here. If a traveling wave solution $e^{j(\omega t-kx)}$ is assumed, the following dispersion relation is obtained.

$$\left[(\bar{\omega}-\bar{k})^2 - \bar{k}^2 G + \frac{\eta}{2}\right]\left[\bar{\omega}^2 - \bar{k}^2 G_1 + \frac{\eta}{2} G_2\right] - \frac{G_2}{4} = 0 \qquad (2)$$

where

$$\bar{\omega} = \frac{\omega}{\omega_{e_1}}, \quad \bar{k} = \frac{kV_o}{\omega_{e_1}}, \quad G = \left(\frac{V_{t_1}}{V_o}\right)^2, \quad G_1 = \left(\frac{V_{t_2}}{V_o}\right)^2, \quad G_2 = \left(\frac{\omega_{e_2}}{\omega_{e_1}}\right)^2$$

Equation (2) is plotted in Fig. 2 for electric field coupling and values of the flow velocity $V_o/V_t \gtrless 2$. For convenience, the stream and structure are assumed to have the same physical constants, so that $V_{t_1} = V_{t_2} = V_t$ and $\omega_{e_1} = \omega_{e_2} = \omega_e$. For $V_o/V_t > 2$, it is evident that there is strong stream-structure coupling only near $k = 0$ and that the coupled system behaves essentially like a stream and structure separately; i.e., it has the static instability of the structure and the convective instability of the stream.[10] This is verified by the Bers-Briggs plot in Fig. 3a where both the saddle point and convective instability are evident. For a slightly supercapillary stream, there is also strong coupling for a passband of wavelengths, and this produces an additional region of instability.

For the magnetically coupled systems, no instabilities are observed for $V_o/V_t < 2$ as can be seen in the dispersion curves of Fig. 4. Again the system exhibits the propagating and envanescent behavior of the uncoupled system. For $V_o/V_t > 2$, however, the system becomes convectively unstable, as illustrated by curves 3 and 4 of Fig. 5.

III The Eigenvalue Problem

Now consider the dynamics with boundaries imposed. The system is a supercapillary jet which enters the interaction region unexcited, and a membrane fixed at the ends.

The boundary conditions consistent with causality are:[10]

$$\xi_1(0,t) = \frac{\partial \xi_1}{\partial x}(0,t) = 0$$

and

$$\xi_2(0,t) = \xi_2(L,t) = 0$$

From Eq. (1) assuming $\xi_{1,2}(x,t) = \mathrm{Re}[\hat{\xi}_{1,2}(x)e^{j\omega t}]$

$$[(j\omega + V_o \frac{d}{d_o})^2 - V_{t_1}^2 \frac{d^2}{dx^2} - \frac{\eta\omega_{e_1}^2}{2}]\hat{\xi}_1 = -\frac{\omega_{e_1}^2}{2}\hat{\xi}_2$$

$$[-\omega^2 - V_{t_2}^2 \frac{d^2}{dx^2} - \frac{\eta\omega_{e_2}^2}{2}]\hat{\xi}_2 = -\frac{\omega_{e_2}^2}{2}\hat{\xi}_1 \qquad (3)$$

The solutions to this system of equations may be written

$$\hat{\xi}_2(x) = \sum_{i=1}^{4} B_i e^{-jk_i x}$$

and

$$\hat{\xi}_1(x) = \sum_{i=1}^{4} Q_i B_i e^{-jk_i x} \qquad (4)$$

where

$$Q_i = -\frac{2}{G_2}[-\bar{\omega}^2 + G_1 \bar{k}_i^2 - \eta \frac{G_2}{2}] \qquad (5)$$

If the boundary conditions are evaluated, the following determinantal equation is obtained.

$$\begin{Bmatrix} 1 & 1 & 1 & 1 \\ e^{-jk_1L} & e^{-jk_2L} & e^{-jk_3L} & e^{-jk_4L} \\ Q_1 & Q_2 & Q_3 & Q_4 \\ k_1Q_1 & k_2Q_2 & k_3Q_3 & k_4Q_4 \end{Bmatrix} \cdot \begin{Bmatrix} B_1 \\ B_2 \\ B_3 \\ B_4 \end{Bmatrix} = 0 \qquad (5)$$

Expanding Eq. (5), we have

$$e^{-j(k_2-k_1)L} \frac{(k_3-k_4)}{(k_2-k_1)} \{\omega^2 + \frac{\eta\omega_{e_2}^2}{2} + V_{t_2}^2 (k_3k_4+k_1K_4+k_1k_3)\}$$

$$+ e^{-j(k_3-k_1)L} \frac{(k_1-k_2)}{(k_3-k_1)} \{\omega^2 + \frac{\eta\omega_{e_2}^2}{2} + V_{t_2}^2 (k_2k_4+k_1k_4+k_1k_2)\} \qquad (6)$$

$$+ e^{-j(k_4-k_1)L} \frac{(k_2-k_3)}{(k_4-k_1)} \{\omega^2 + \frac{\eta\omega_{e_2}^2}{2} + V_{t_2}^2 (k_2k_3+k_1k_3+k_1k_4)\} = 0$$

Equation (6), combined with the dispersion relation, Eq. (2), forms the eigenvalue equation to be solved.

Electric Coupling

The eigenfrequencies for electric field coupling are shown in Fig. 6 for the lowest three modes using the experimental values of the parameters.[9]

To interpret the curves, it is useful to compare the eigenfrequencies for the uncoupled case, namely a single structure field coupled to rigid plates. The determinantal equation reduces simply to $k = \frac{n\pi}{L}$ and the eigenvalue equation becomes

$$(\omega/\omega_{e_1})^2 = G_1\left(\frac{n\pi V_o}{L\omega_{e_1}}\right)^2 - \frac{\eta}{2} G_2 \qquad (7)$$

The real parts of the eigenfrequencies shown in Fig. 6 are essentially those of the structure alone, (Eq. 7) field coupled to a rigid wall. In addition, the point of instability for the first mode is nearly that predicted by Eq. (7). The principle effect of the mutual coupling is to produce electrical damping of the wave below the point of instability. Above the instability point the growth rate also agrees quite well with the uncoupled case and approaches the same asymptotic limit. The decay branch, however, exhibits an increased decay rate.

The effect of the coupling on mode 2, however, is quite significant. Mode 2 exhibits overstability for a wide range of $\frac{L\omega_e}{V_o}$, and becomes unstable (assuming no mechanical or electrical losses) as soon as the slightest electric field is applied. As $\frac{L\omega_e}{V_o}$ is increased, the normalized growth rate increases to quite a large value until the real part of the eigenfrequency becomes zero and the curve splits into two statically unstable modes (not shown). The deviation from the mutually uncoupled eigenfrequency case becomes large with increasing $\frac{L\omega_e}{V_o}$. The overstable behavior of mode 2 is exhibited by higher modes as well.

The eigenfunctions may be computed using Eqs. (2), (4), and (6). If we assume $B_1 \neq 0$ for the moment, then the ratios of the coefficients to B_1 may be computed from

$$\begin{Bmatrix} 1 & 1 & 1 \\ Q_2 & Q_3 & Q_4 \\ k_2Q_2 & k_3Q_3 & k_4Q_4 \end{Bmatrix} \cdot \begin{Bmatrix} \frac{B_2}{B_1} \\ \frac{B_3}{B_1} \\ \frac{B_4}{B_1} \end{Bmatrix} = \begin{Bmatrix} -1 \\ -Q_1 \\ -Q_1k_1 \end{Bmatrix} \qquad (8)$$

Since B_1 is arbitrary, it may be set equal to the determinant of the coefficient matrix of Eq. (8). This allows the B's to be written in a symmetric form and the restriction that $B_1 \neq 0$ can be removed. Manipulating Eq. (8) we get

$$\begin{aligned}
B_1 &= (k_3-k_4)(k_3-k_2)(k_4-k_2)\ \{A + V_{t_2}^{\ 2}\ (k_3k_4+k_3k_2+k_4k_2)\} \\
B_2 &= (k_4-k_3)(k_4-k_1)(k_3-k_1)\ \{A + V_{t_2}^{\ 2}\ (k_3k_4+k_1k_3+k_1k_4)\} \\
B_3 &= (k_2-k_4)(k_2-k_1)(k_4-k_1)\ \{A + V_{t_2}^{\ 2}\ (k_4k_2+k_4k_1+k_2k_1)\} \\
B_4 &= (k_3-k_4)(k_3-k_1)(k_2-k_1)\ \{A + V_{t_2}^{\ 2}\ (k_3k_2+k_3k_1+k_2k_1)\}
\end{aligned} \tag{9}$$

where $A = \omega^2 + \dfrac{\tau\omega_{e_2}^{\ 2}}{2}$.

From Eq. (4) the spatial dependence of the eigenfunctions can be calculated and finally the time dependent eigenfunctions follow from

$$\xi(x,t) = \mathrm{Re}[\xi(x)e^{j\omega t}]$$

Typical eigenfunctions for the lowest modes of the stream structure system for the case $\omega_{e_1} = \omega_{e_2} = \omega_e$, $V_{t_1} = V_{t_2} = V_t$ and $V_o/V_t = 2$ are shown in Fig. 7. The fundamental mode for both the growth and decay branches exhibits the behavior of the mutually uncoupled jet and spring. The relative phasing is as expected, since a downward deflection of the spring weakens the field in the midregion and produces an upward traction on the jet. The peak amplitude of the membrane is very slightly shifted downstream. The membrane eigenfunction of mode 2 is also the same as in the mutually uncoupled case. For $x < \frac{L}{2}$ the traction on the jet is downward; for $\frac{L}{2} < x < L$, upward. But a certain length is required for the jet to reverse its direction of motion and cross the axis. The amplitude grows fairly rapidly since the self and mutual coupling terms are reinforcing.

Magnetic Coupling

The magnetic field coupled system eigenfrequencies for the same parameters as in the case just mentioned are shown in Fig. 8 for the lowest three modes. The real parts of the eigenfrequencies are typical of a magnetically coupled membrane.[11] The imaginary parts exhibit the same decay of the fundamental mode and growth of higher modes as for electric field coupling. It is interesting that each higher mode exhibits a peak growth rate, the second mode for $\frac{L\omega_h}{V_o} = 2.6$ and the third mode for $\frac{L\omega_h}{V_o} \approx 3.9$. The maximum growth rates are about equal. This implies an optimum length if one wished to design an oscillator using a particular mode (neglecting the adverse effects of other modes). That such a peak should occur is reasonable if one recalls from Fig. 3 that no absolute instabilities exist in the infinite system.

The eigenfunctions for $\frac{L\omega_h}{V_o} = 1.75$ are shown for the three lowest modes in Fig. 9. The same membrane-like behavior is observed as in the electric field case, but the jet behavior is more wavelike. Since the magnetic self coupling term has a stabilizing effect, the field coupled jet by itself exhibits purely propagating waves. By contrast the electric field coupled jet exhibited convective instability in the absence of mutual coupling.

It is evident from the previous discussion of electric and magnetic field stream-structure interactions that the electric and magnetic systems have many common features. The same conclusion was reached in (9) in the discussion of counter-streaming jets, where it was found that the mutual coupling and convective terms were of primary importance, with the surface tension unimportant, and the self coupling term either enhanced (electric field) or depressed (magnetic field) instabilities.

It is worthwhile to speculate if the dynamical terms in the equations of motion play the same role in the present case.

The Degenerate System

Let us postulate here that the jet is without surface tension and that the self coupling field terms are unimportant. (This involves setting G and η to zero). As a result the electric and magnetic systems yield the same eigenfrequency curves (replacing ω_e^2 by $-\omega_h^2$ leaves Eq. (2) unchanged). Since the right hand sides of Eq. (3) change sign however, the eigenfunctions are different. This can be expected physically since an upward displacement of the structure, say, will exert a downward traction on the stream for electric field coupling and an upward traction in the magnetic case . The resulting eigenfrequency curves (Fig. 10) appear to be a hybrid of the electric and magnetic field cases (compare Fig. 10 with Figs. 6 and 8. Strictly speaking, the comparison is not valid, but the results are qualitatively insensitive to changes in parameters).

The degenerate system exhibits damping of the fundamental mode and overstability in the higher modes characteristic of both types of field coupling. It also exhibits static instabilities characterisitic of electric field coupling.

From the above discussion, several facts become clear concerning field coupled stream - structure systems:

1. The real part of the eigenfrequencies can be predicted quite accurately assuming the stream to be a rigid wall, for all $\frac{L\omega_{e,h}}{V_o}$ from Eq. (7).

2. The imaginary part of the eigenfrequency can also be approximately predicted from the structure alone in the limit $\frac{L\omega_{e,h}}{V_o} \to \infty$.

3. The fundamental mode is damped by the stream (below a critical value of $\frac{L\omega_e}{V_o}$ for the electric case) and all higher modes exhibit overstability for both types of coupling.

We may conclude, as also pointed out in (9) for counter-streaming jets, that the mutual coupling term is of fundamental importance. This instability is produced by the supercapillary stream, since the magnetic system exhibits no instabilities if the stream velocity is zero or even subcapillary.

The role of the self coupling terms is now apparent. For electric field coupling, self coupling is destabilizing; the most important effect is to enhance the growth rate of existing instabilities. For the magnetic case the magnetic field is stabilizing and is sufficient to suppress the static instability of the fundamental mode and reduce, although not suppress the growth rate of the overstabilities.

IV. Physical Explanation of Stream-Structure Overstability

It is possible to describe the overstability simply in terms of motions of elements of fluid interacting with the structure. Two ingredients are essential: (1) there must be time average power flow from stream to the structure; (2) even if the stream supplies net power, the mechanism must be present for the structure to feed back some of the downstream absorbed power to the upstream section of the stream to sustain the oscillations. Otherwise the system behaves as an amplifier and not an oscillator. To simplify the discussion, surface tension on the stream will be ignored and the only force acting on the fluid elements to be studied is due to mutual coupling.

It will be assumed for the convenience of the argument that the stream velocity is twice the wave velocity on the structure, or alternately, the transit time of the jet is half the period of oscillation. Consider an element of fluid A which enters the interaction region unexcited at $t = 0$ with the spring at half amplitude and rising (Fig. 11). As ωt advances to $\pi/4$, the structure exerts a strong downward traction on A as it travels the half-length of the system, but has supplied only a modest amount of power because of the small transverse stream velocity. During the second quarter period element A exerts an upward traction on the structure, and further, this upward force occurs at a time when the structure is at near maximum upward velocity, so that the kinetic energy transfer from the fluid to the structure is large, much larger than that delivered to element A during the first quarter cycle. Thus A at least satisfies both requirements for overstability. It is necessary, however, to show that other fluid elements do not degrade the overstable effect of element A. Following other particles at different entrance times, one concludes that elements like A in fact characterize the system. The argument may be extended to the third or higher modes without conceptual difficulty, although the details become involved.

In all of the modes higher than the first, the mechanism for instability depends on the structure exciting the jet upstream and the jet in turn transferring net power back to the structure. The fundamental mode is peculiar, however, since each point on the spring has the same phase, and no feedback mechanism is available. Hence the fundamental mode is not overstable.

V. An Electrohydrodynamic Experiment

To investigate some of the ideas presented in the foregoing sections, an electrohydrodynamic experiment was constructed consisting of a circular water jet and a weak metal spring of the same dimensions, supported in the horizontal plane. Two external plates provided the same equilibrium electric stress on each side of the jet and spring. The apparatus was as shown schematically in Fig. 1. For convenience the jet was grounded. Only one voltage source was required since the outer plates were carefully adjusted so that the spring and jet did not deflect when the field was turned on. Since the theoretical model assumes a planar geometry, it was necessary that the system parameters be measured. This was done by replacing the jet by a second matched spring and measuring resonant frequency vs. voltage for the fundamental symmetric and antisymmetric modes. (The procedure and results are described in (9) and (10)). So that the elements be coplanar, the plates were bent and the spring supported by fine insulating strings to match the curvature of the jet. The strings, however, introduced an additional restoring force on the spring, acting like a distributed set of pendulums, and this effect is included in the analysis.

To detect the existance of absolute instabilities, the d.c. voltage was increased from zero until either an instability or electrical breakdown occurred. At low voltages, the spring and jet were effectively uncoupled, disturbances on the spring appeared as standing wave oscillations which decayed slowly in time, while jet disturbances appeared as pulses traveling downstream at about the jet velocity. As the voltage was increased, the spring and jet began to interact. The oscillation frequencies of the spring were not affected appreciably

by the presence of the electric field; the damping, however, was significantly altered. The fundamental mode decayed more rapidly while higher modes decayed more slowly. Disturbances on the jet exhibited spatial growth for long waves (characteristic of a single jet field coupled to rigid plates).

As the voltage was increased further, a critical electric field was reached when the system spontaneously broke into oscillation and the amplitudes increased slowly with time, building up to such an amplitude that the spring and jet collided, terminating the experiment. The trajectory of the spring was the third mode. The jet, however, exhibited a traveling wave behavior with an exponential envelope which grew in time at the same rate as the spring. The critical voltage was reproducible. If this voltage were exceeded by a modest amount, the system became overstable, but the spatial character of the deflections was unchanged. Further increase of the voltage resulted in other modes becoming unstable, first the fourth mode, then others.

In order to examine the eigenfrequencies quantitatively, each of the lowest four modes was excited and the resulting complex eigenfrequency recorded as a function of voltage. The modes were excited by segmenting the plate adjacent to the spring and applying a small AC voltage at the resonant frequency. This driving voltage was spatially periodic with the wavelength of the disturbance on the spring. The excitation was then removed and the decay (or growth) of the mode recorded. In this way both the real and imaginary parts of the eigenfrequency were measured.

The theoretical values of the real part of the resonant frequencies at zero voltage should be exact multiples of the fundamental if we ignore

the effect of the support strings on the spring. This, however, was not observed, as seen in Fig. 12 (resonant frequency measurements are accurate to $\pm$ .01 cps, so that the deviation from a straight line in Fig. 12 is significant).

Consider that the spring experiences a continuum gravitational restoring force through the support strings holding the spring. The restoring force on a section of spring of unit length is simply given by $-\frac{\rho_\ell g}{\ell}$ (ρ_ℓ is the lineal density of the spring.) Since the ends of the spring are fixed, $k = \frac{n\pi}{\ell}$ and the functional dependence of the frequency on mode number for zero electric field becomes

$$f^2 = an^2 + b \qquad (10)$$

The parameters a and b were calculated from the data and Eq. (10) drawn as the solid curve of Fig. 12.

The appliation of the voltage had the effect of reducing the real part of the fundamental eigenfrequency slightly while having virtually no effect on higher modes, as predicted by theory. The important effect was on the decay or growth rate. In Fig. 13 a-d the experimental and theoretical results are shown. The solid unmarked curves are the theoretical curves shifted down by an amount equal to the damping at zero electric field. This shift represents mechanical loss in the system, primarily due to air drag. The fundamental mode does indeed decay and the next three modes show overstable behavior within the limits of the experiment. One point was taken with the system overstable (Mode 3). Because Mode 3 became unstable at 12kv, it was not possible to take measurements on any of the other modes beyond this point.

Inspection of the zero field damping correction shows the damping increases with frequency. Simple calculations of air drag for an oscillating spring and jet indicate the same dependence on frequency and approximately the correct magnitude.(10)

In order to photograph the overstability a second apparatus was constructed with the elements mounted in a vertical plane. The transverse spacing was increased and the longitudinal dimension shortened. It was found necessary to perform the experiment in an atmosphere of Freon to prevent corona discharge and breakdown. As the voltage was raised to the critical point, the system became unstable as before, but now the first unstable mode was the second mode. Figure 14 was photographed with a shutter speed adjusted to the period of oscillation to show the amplitude envelope.

High speed motion pictures* were taken to observe the phase relationships of the spring and jet during an oscillation and to observe the oscillation buildup. A sequence of four frames one sixth of a cycle apart in time are shown in Fig. 15. The second natural mode of the spring and the spatially growing character of the jet (at the same frequency as the spring) are apparent. The relationship of the jet deformation to that of the spring lends support to the physical arguments of the previous section concerning the mechanism for overstability.

To the best of the author's knowledge, this is the first stream-structure device which couples a convecting fluid exhibiting amplifying

---

* These motion pictures were taken by Educational Services, Inc., Watertown, Mass., for use in a film by J. R. Melcher, sponsored by the National Science Foundation under the supervision of the National Committee on Electrical Engineering Films.

waves in the uncoupled state to a passive propagating structure to produce overstabilities. The time dependent eigenfunctions, computed for the experimental conditions and for the time sequence shown in Fig. 15a, provide an excellent picture of the dynamics, as can be seen by a comparison of Fig. 16 with the photographs.

VI Conclusions

The problem of describing the dynamics of a fluid stream coupled to a flexible structure with the system bounded in both the transverse and longitudinal directions is formidable without simplifying assumptions. The effect of surface tension or elastic tension is to stabilize short waves, while at the same time the field coupling of the stream and structure to each other and to the transverse plates is strongest at the longest wavelengths. Thus the dynamics of the coupled system is determined by the behavior of long waves, and the longitudinal boundaries have been carefully considered in the present paper. Because the coupled equations are hyperbolic, real characteristics exist and causal boundary conditions can be unambiguously specified (for the present problem two upstream conditions on the jet and one upstream and one downstream on the structure).

The dispersion relation and Bers-Briggs stability criterion give considerable insight as to system stability when the ends are far apart, but it is not too surprising that these results are unreliable as the ends become closer together, and it becomes unecessary to carry out the detailed calculations of the eigenfreqqencies. Furthermore, the Bers-Briggs criterion offers no information concerning the details of any particular mode.

For example the Bers-Briggs criterion predicts static instability for the electric field system, no absolute (static)instabilities for the magnetic system, and convective instabilities for both types of coupling. The static instability is observed also in the finite length electric field system, but now both systems exhibit overstability. One might ask the question as t_o whether a convective instability has meaning in a system which is truly bounded. The downstream boundary in effect fixes the wavenumbers and converts the convective instability into an overstability.

Finally, as pointed out in (9), there is a close analogy between the magnetic field coupled systems and electron beam devices. The present stream-structure device is analogous to an extended region klystron, where the conducting jet is replaced by an electron beam and the membrane by a cavity. A few calculations have indicated that this finite length system exhibits overstabilities similar to those shown in Fig. 8.

Acknowledgements

I wish to express my sincere thanks to Professor James R. Melcher of MIT for his guidance and help throughout the course of this work. Mr. Felipe Herba's assistance was most helpful in carrying out the experiments. This research was performed under NASA Contract NsG-368. The numerical work was done at the MIT Computation Center.

Figure Captions

Figure 1. A highly conducting fluid stream moving to the right with velocity V_o is field coupled to a highly conducting elastic structure.

Figure 2. Dispersion curves, assuming solutions of the form exp $j(\omega t-kx)$ for the long wave model ($\lambda >> a$) of the system in Figure 1(a), electric field coupling. Complex ω has been plotted for real k. Curves (a) and (c), with the mutual coupling ignored, have been included for comparison purposes.

Figure 3. Stability curves for electric field coupling for the conditions of Figure 2(b) and (d). Complex k is plotted for fixed ω_r as ω_i is increased from $-\infty$ to 0. Saddle points are apparant in both figures for the 1 curves, indicating a static-type absolute instability.

Figure 4. Dispersion curves similar to Figure 2 for magnetic field coupling. Complex ω has been plotted for real k. Curves (a) and (c), with the mutual coupling ignored, have been included for comparison purposes. No instabilities are observed for $V_{o1}/V_t < 2$.

Figure 5. Stability curves for magnetic field coupling, corresponding to the dispersion curve of Figure 4(d). A convective instability is exhibited by curves 3 and 4.

Figure 6. Complex eigenfrequency vs. normalized length for experimental conditions showing the lowest three modes. The real part of the eigenfrequency is symmetric about the abscissa. The fundamental mode is damped for $L\,\omega_e/V_o < 3.4$ and exhibits static instability for larger $L\,\omega_e/V_o$. Higher modes exhibit overstability for a wide range of $L\,\omega_e/V_o$.

Figure Captions Continued

Figure 7. Typical eigenfunctions for the two lowest modes, electric field coupling. The elastic structure (spring) deflection is predominantly sinusoidal and the jet deflection sinusoidal with an exponential envelope characteristic of the two elements acting independently.

Figure 8. Complex eigenfrequency vs. normalized length for a magnetic field coupled stream-structure system for the lowest three modes. The fundamental mode exhibits decay while higher modes are overstable for a wide range of $L\omega_e/V_o$. The conditions are the same is in Figure 4(d).

Figure 9. Eigenfunctions for the three lowest modes for the magnetic field coupled system of Figure 8. The eigenfunctions are similar to those of Figure 7, except for a 180° phase inversion of the elastic structure in the two systems. This illustrates the antiduality of magnetic and electric field coupling.

Figure 10. Complex eigenfrequency vs. normalized length for the degenerate field coupled stream-structure system. Fluid surface tension and the field self coupling terms have been neglected to illustrate the importance of the mutual coupling in producing overstability.

Figure 11. Illustration of the feedback mechanism producing overstability.

Figure 12. Experimental eigenfrequency vs. mode number for zero applied voltage. The deviation from a straight line is caused by the effect of the support strings on the elastic structure (spring).

Figure Captions Continued

Figure 13. Imaginary part of eigenfrequency vs. applied voltage for the lowest four modes. The lower solid curve is the theoretical curve corrected for the mechanical damping at zero voltage. The instability of the third mode is apparent in (c).

Figure 14. Time exposure for one period of oscillation during build-up of electric field coupled streaming overstability. Spring (left) and jet (right) are resonating at the second eigenfrequency.

Figure 15. High speed photographs of the streaming overstability in Figure 14. The time interval between exposures is about 60° in phase. The frequency of oscillation is about 7 cps.

Figure 16. Theoretical eigenfunctions for the experimental conditions of Figure 15.

References

1. Fung, Y. C., AIAA Journal 1, 898 (1963).
2. Dugundji, J. and Ghareeb, N., AIEE Journal 3, 1126 (1965).
3. Pierce, J. R., Traveling Wave Tubes, Van Nostrand (1950) Ch. 4.
4. Haus, H. A., J. Appl. Phys. 33, 2161 (1962).
5. Rayleigh, J. W. S., The Theory of Sound Vol. II, Dover (1945), Ch. 20.
6. Dugundji, J., MIT Aero. and Structures Res. Lab. AFOSR 65-1907 (Aug. 1965).
7. Bers, A., and Briggs, R., QPR No. 71, Res. Lab. of Electronics, MIT, pp. 122-130 (Oct. 1963).
8. Briggs, R., Electron Stream Interactions with Plasmas, The MIT Press (1964).
9. Ketterer, F. D. (to be published).
10. Ketterer, F. D., PhD Thesis, Dept. of Electrical Engineering, MIT (Sept. 1965).
11. Melcher, J. R., Field Coupled Surface Waves, The MIT Press (1963).

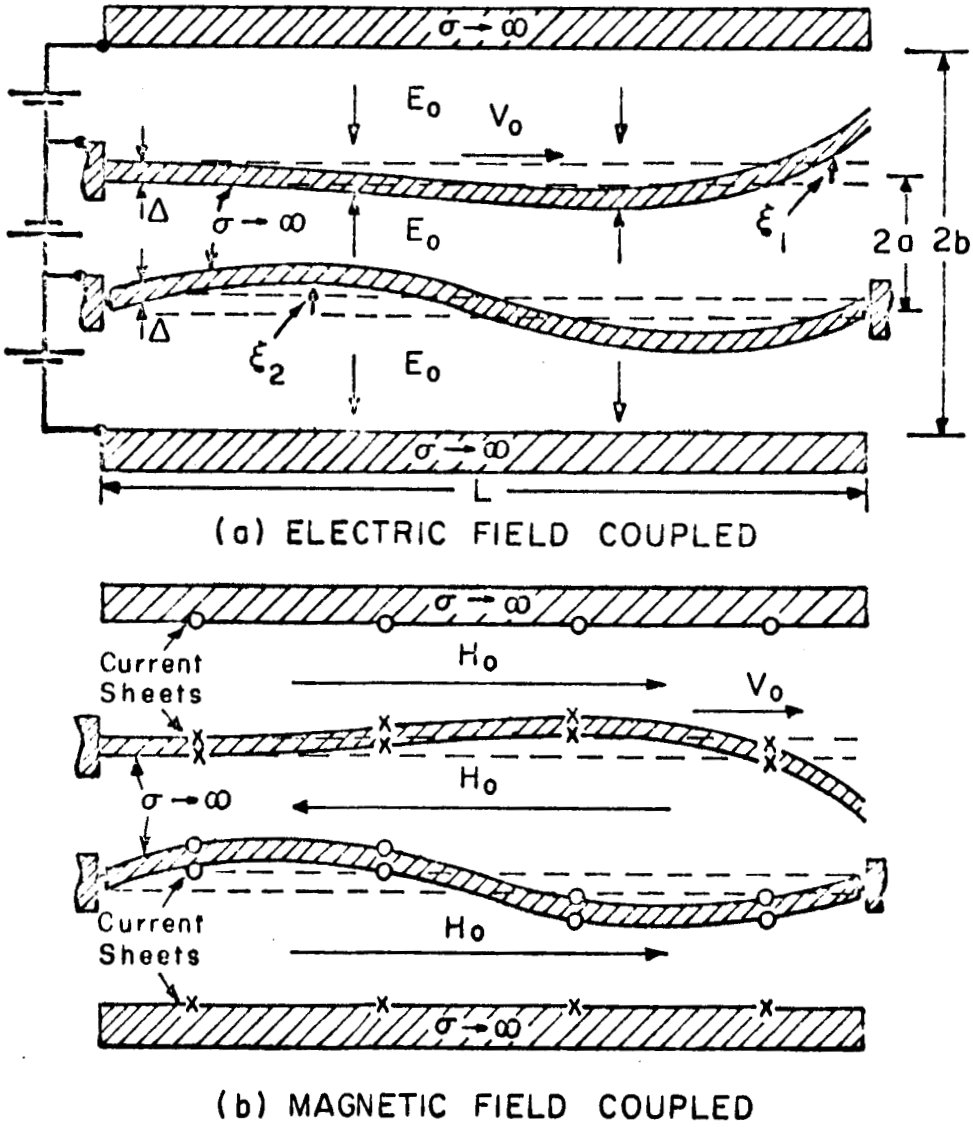

Figure 1. A highly conducting fluid stream moving to the right with velocity V_o is field coupled to a highly conducting elastic structure.

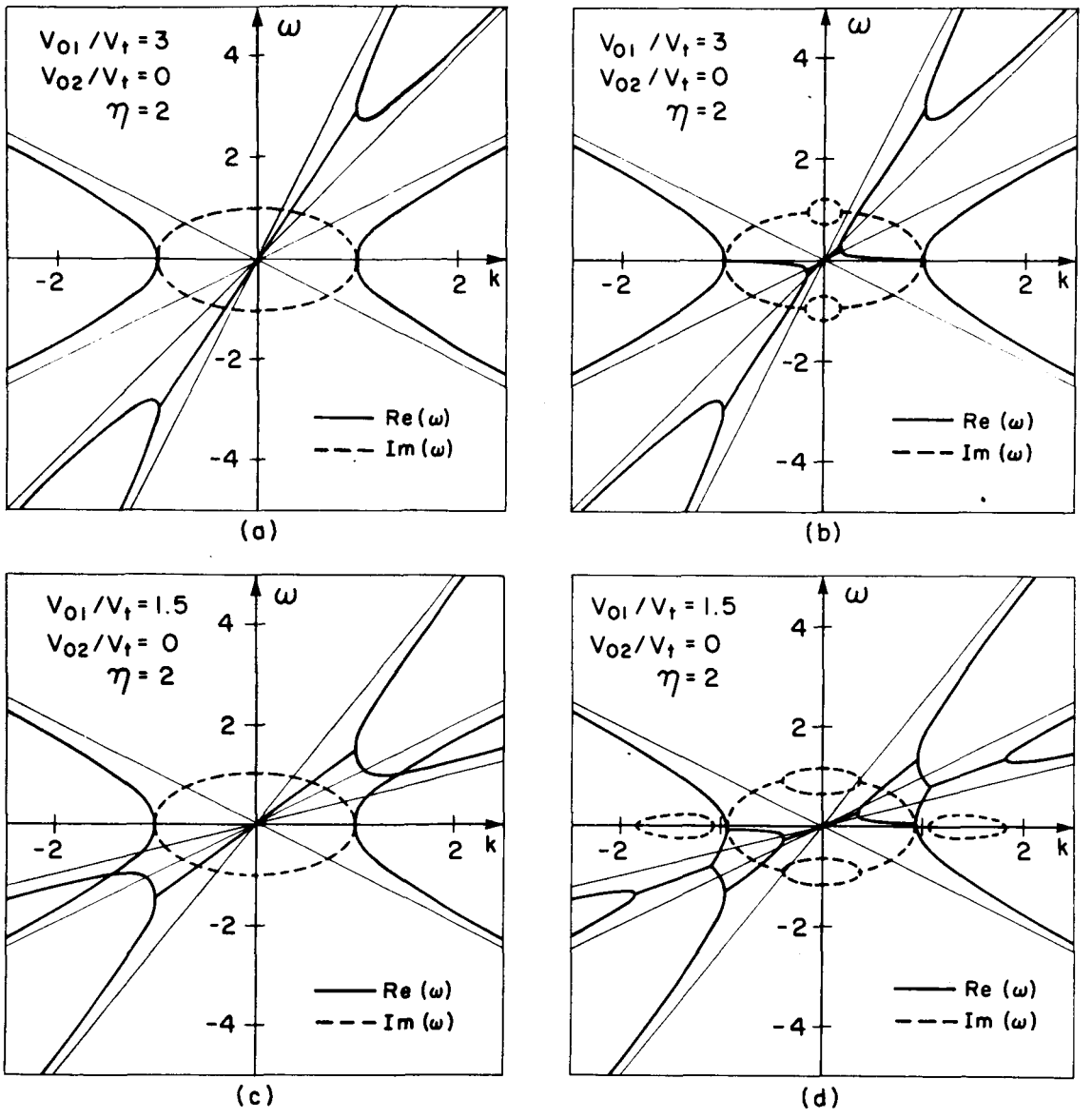

Figure 2. Dispersion curves, assuming solutions of the form exp $j(\omega t - kx)$ for the long wave model ($\lambda >> a$) of the system in Figure 1(a), electric field coupling. Complex ω has been plotted for real k. Curves (a) and (c), with the mutual coupling ignored, have been included for comparison purposes.

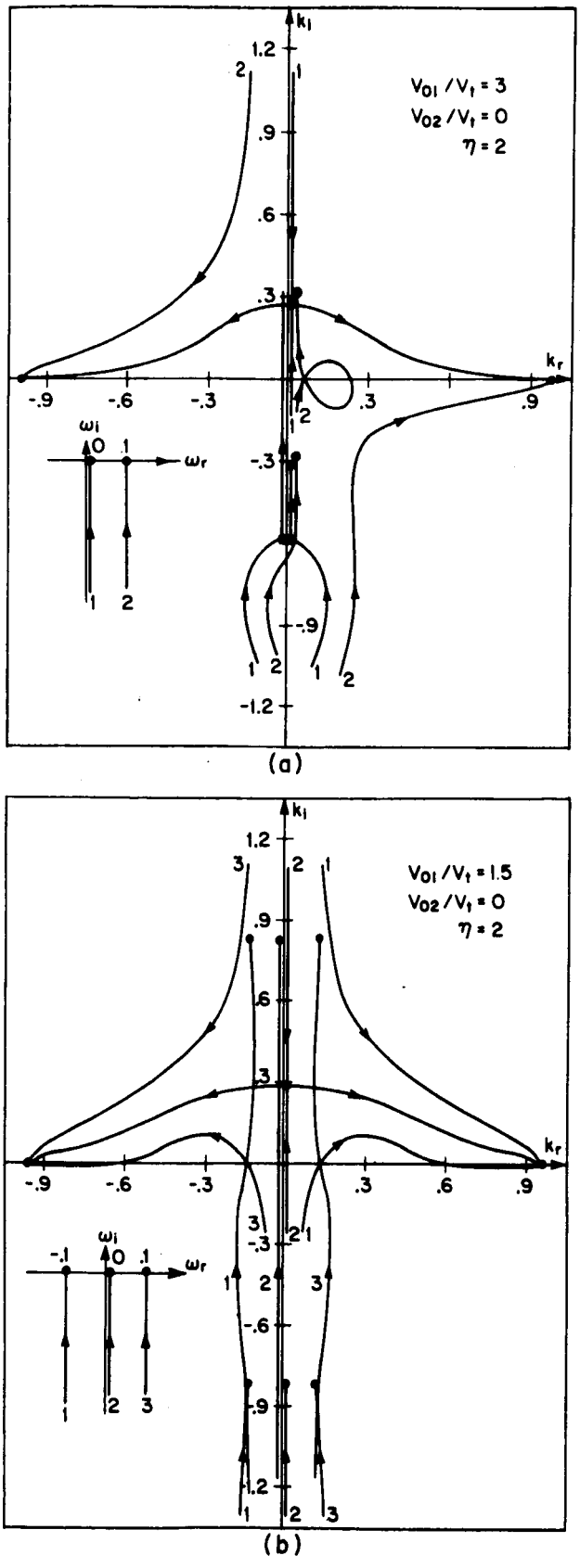

Figure 3. Stability curves for electric field coupling for the conditions of Figure 2(b) and (d). Complex k is plotted for fixed ω_r as ω_i is increased from $-\infty$ to 0. Saddle points are apparant in both figures for the 1 curves, indicating a static-type absolute instability.

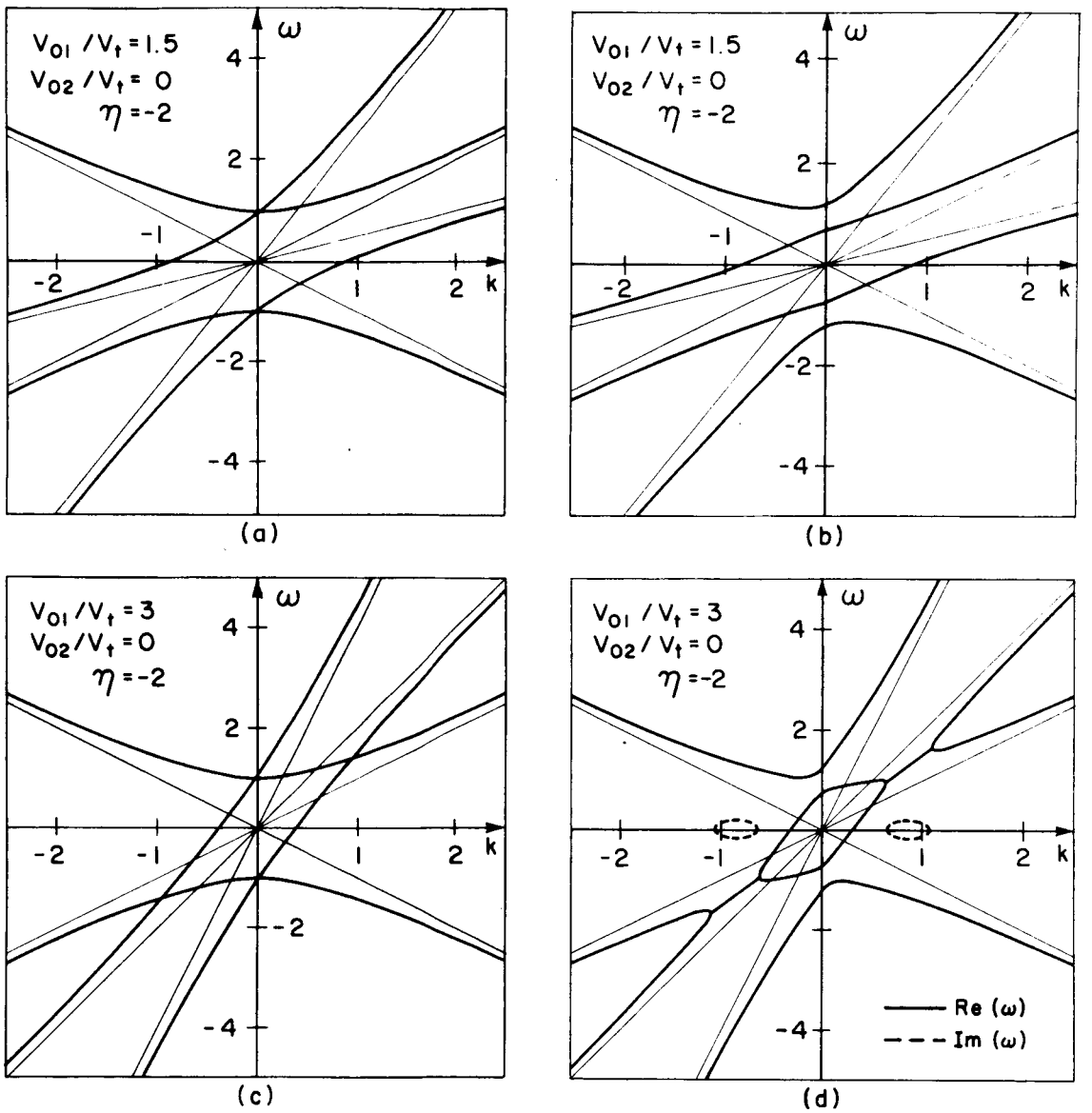

Figure 4. Dispersion curves similar to Figure 2 for magnetic field coupling. Complex ω has been plotted for real k. Curves (a) and (c), with the mutual coupling ignored, have been included for comparison purposes. No instabilities are observed for $V_{01}/V_t < 2$.

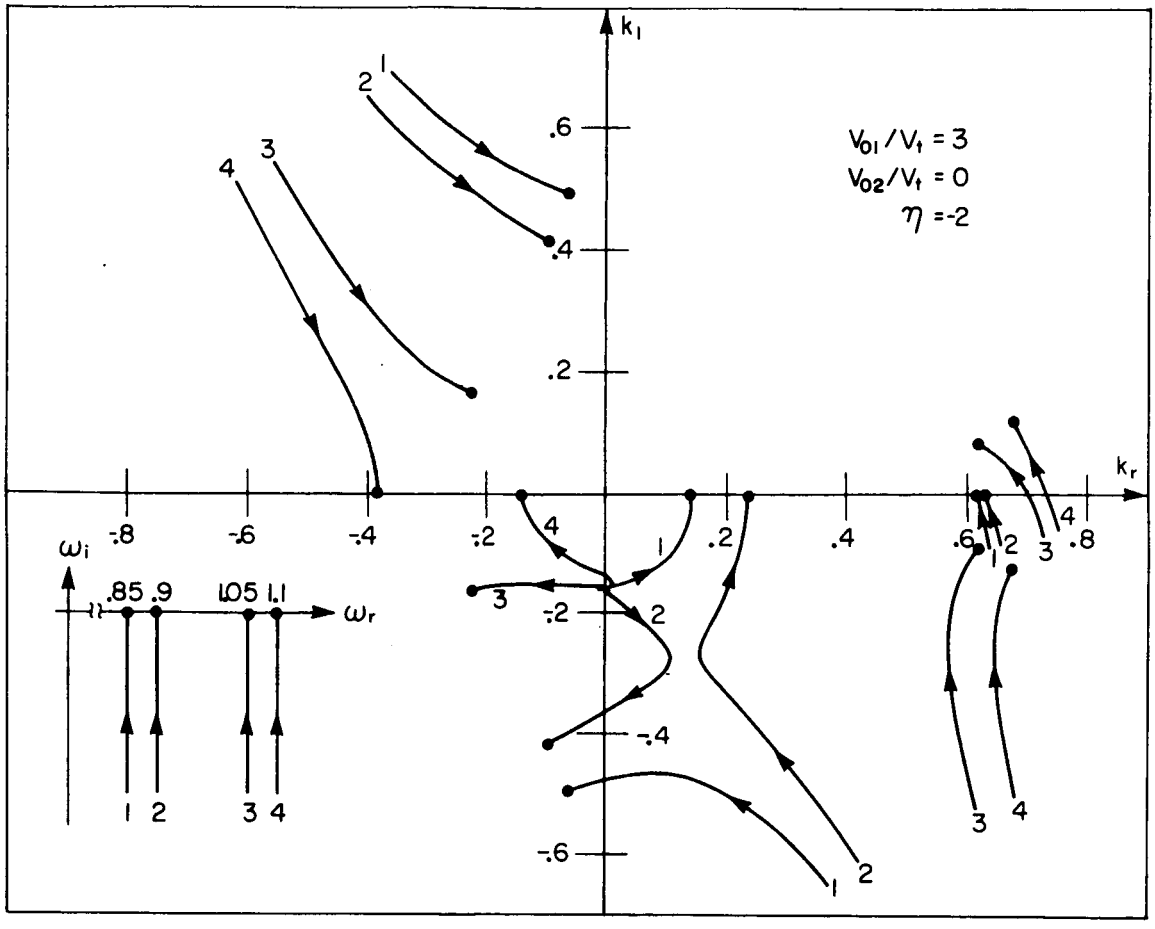

Figure 5. Stability curves for magnetic field coupling, corresponding to the dispersion curve of Figure 4(d). A convective instability is exhibited by curves 3 and 4.

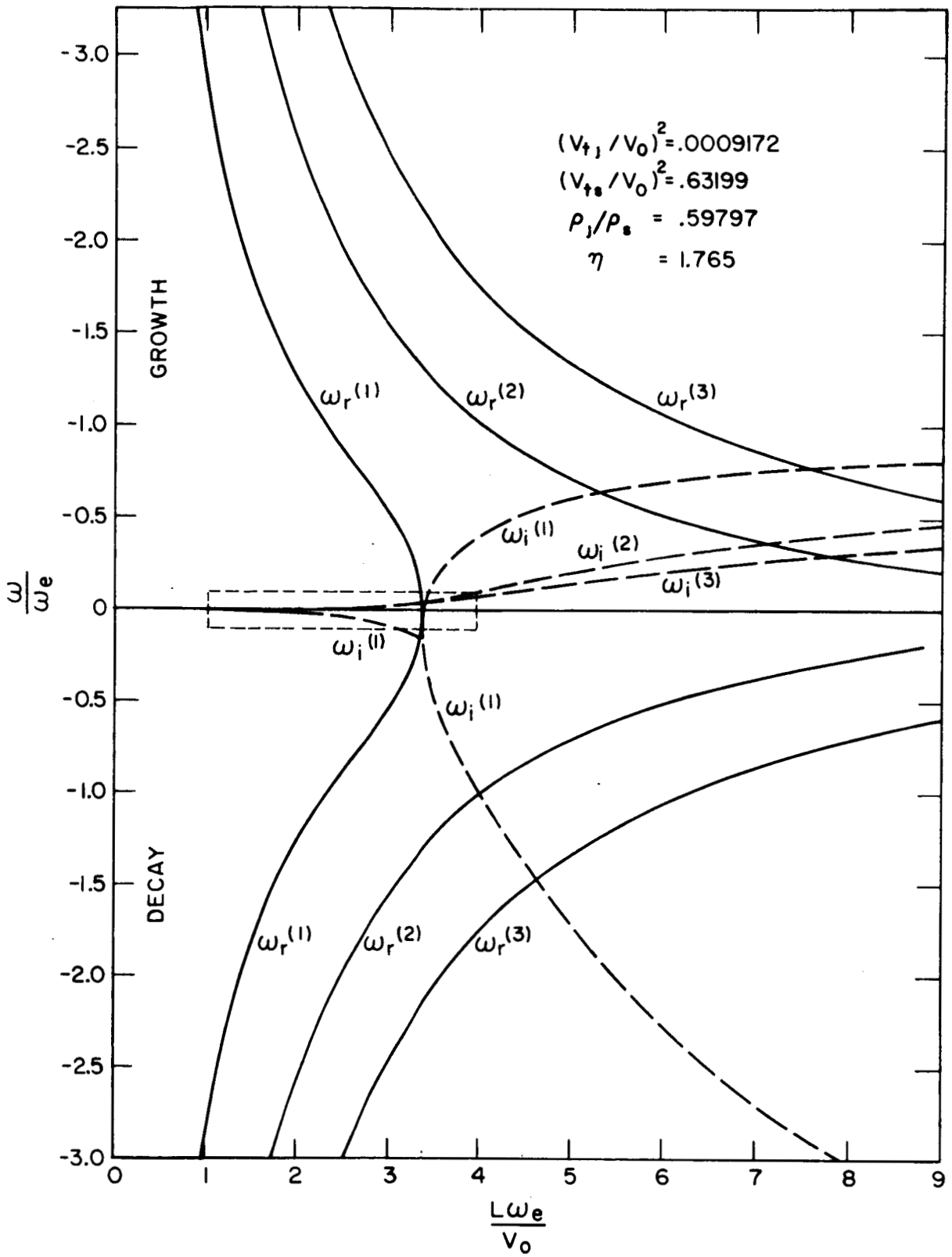

Figure 6. Complex eigenfrequency vs. normalized length for experimental conditions showing the lowest three modes. The real part of the eigenfrequency is symmetric about the abscissa. The fundamental mode is damped for $L\,\omega_e/V_o < 3.4$ and exhibits static instability for larger $L\,\omega_e/V_o$. Higher modes exhibit overstability for a wide range of $L\,\omega_e/V_o$.

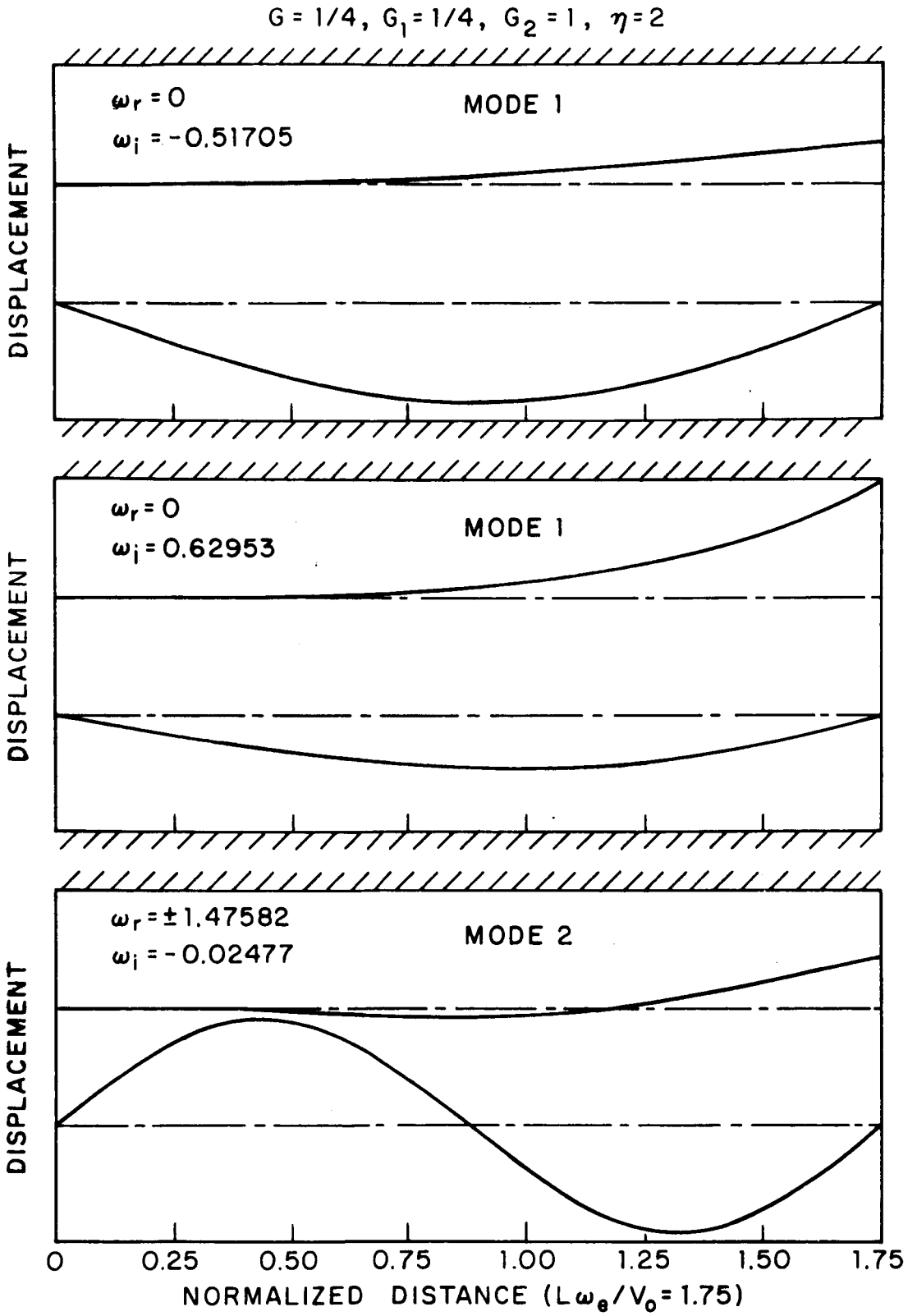

Figure 7. Typical eigenfunctions for the two lowest modes, electric field coupling. The elastic structure (spring) deflection is predominantly sinusoidal and the jet deflection sinusoidal with an exponential envelope characteristic of the two elements acting independently.

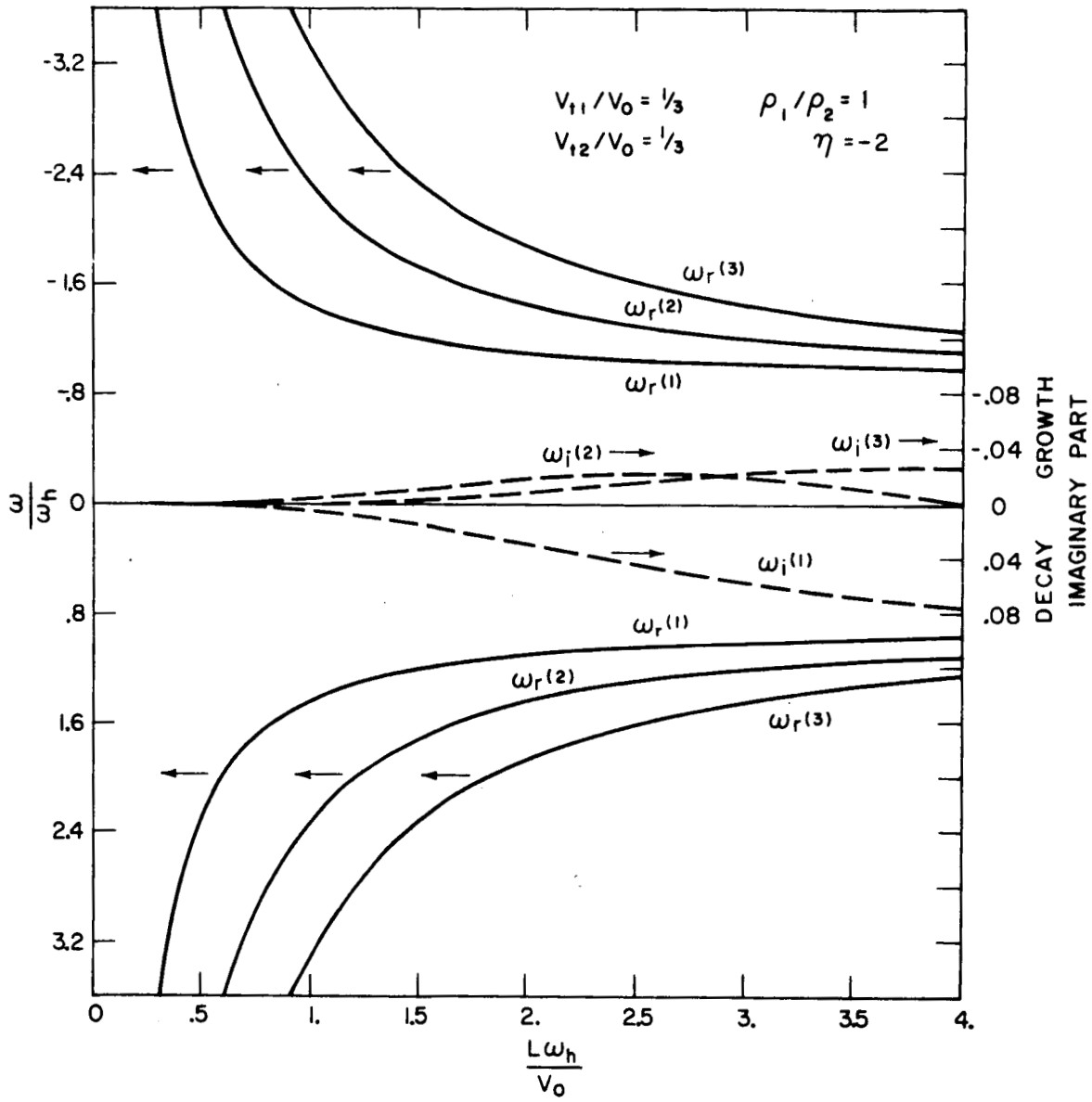

Figure 8. Complex eigenfrequency vs. normalized length for a magnetic field coupled stream-structure system for the lowest three modes. The fundamental mode exhibits decay while higher modes are overstable for a wide range of $L\omega_e/V_o$. The conditions are the same is in Figure 4(d).

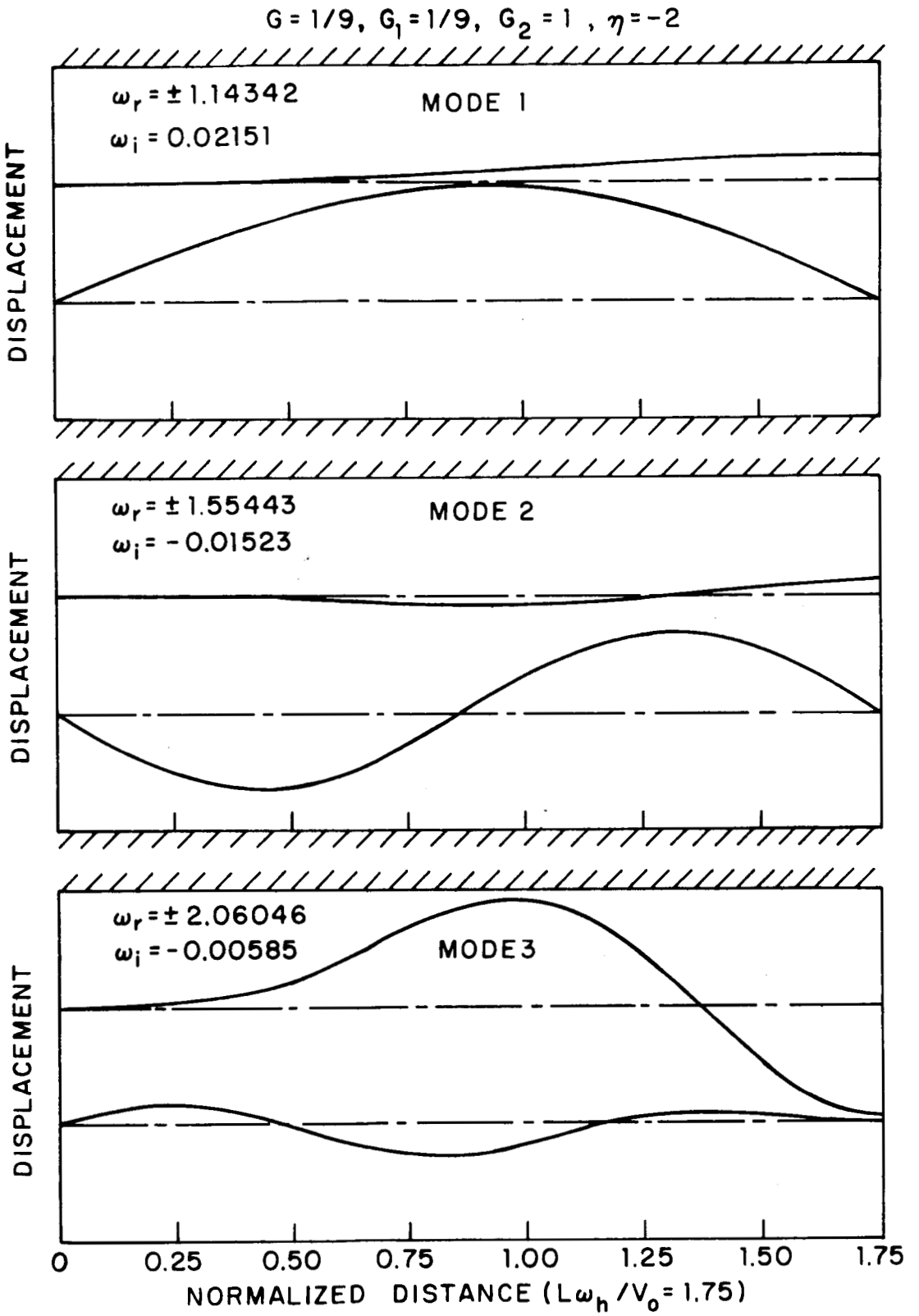

Figure 9. Eigenfunctions for the three lowest modes for the magnetic field coupled system of Figure 8. The eigenfunctions are similar to those of Figure 7, except for a 180° phase inversion of the elastic structure in the two systems. This illustrates the antiduality of magnetic and electric field coupling.

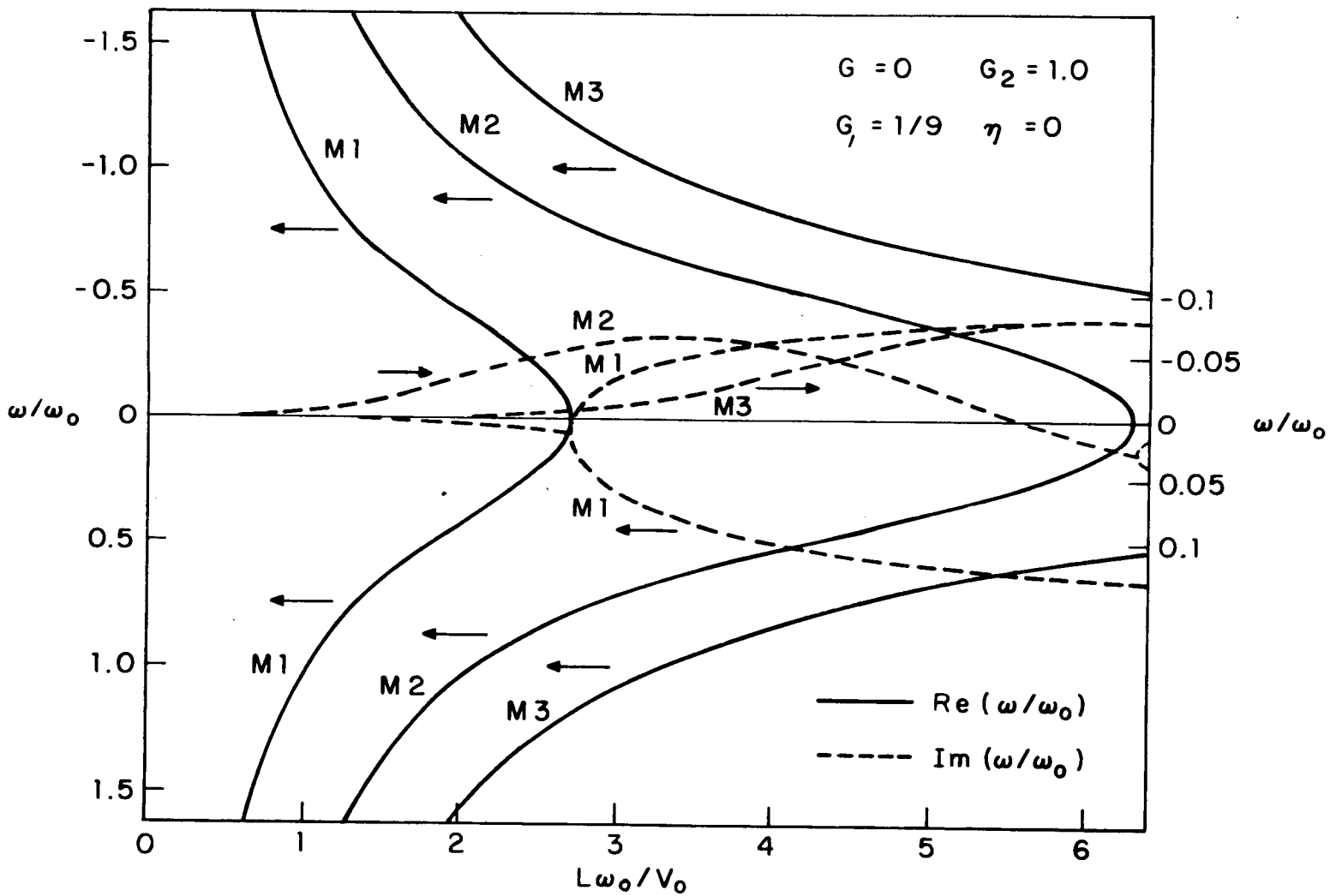

Figure 10. Complex eigenfrequency vs. normalized length for the degenerate field coupled stream-structure system. Fluid surface tension and the field self coupling terms have been neglected to illustrate the importance of the mutual coupling in producing overstability.

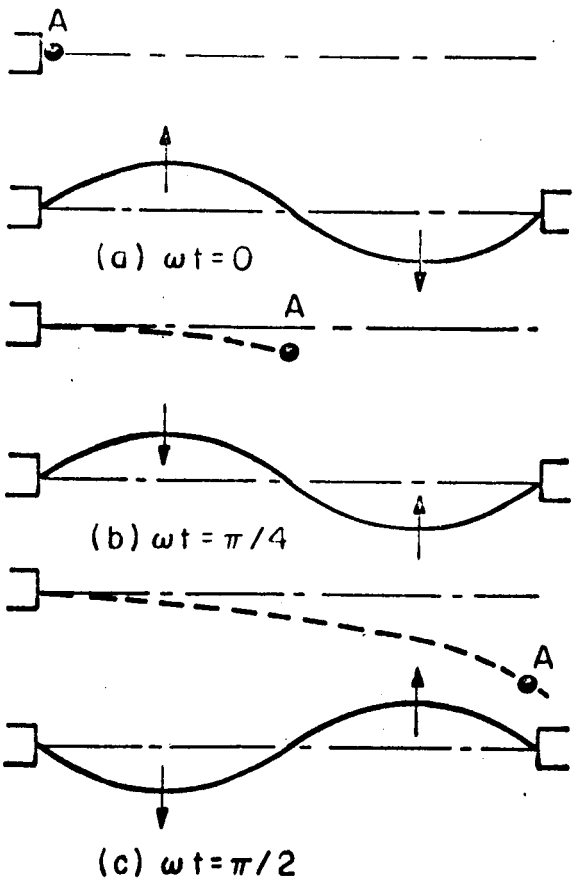

Figure 11. Illustration of the feedback mechanism producing overstability.

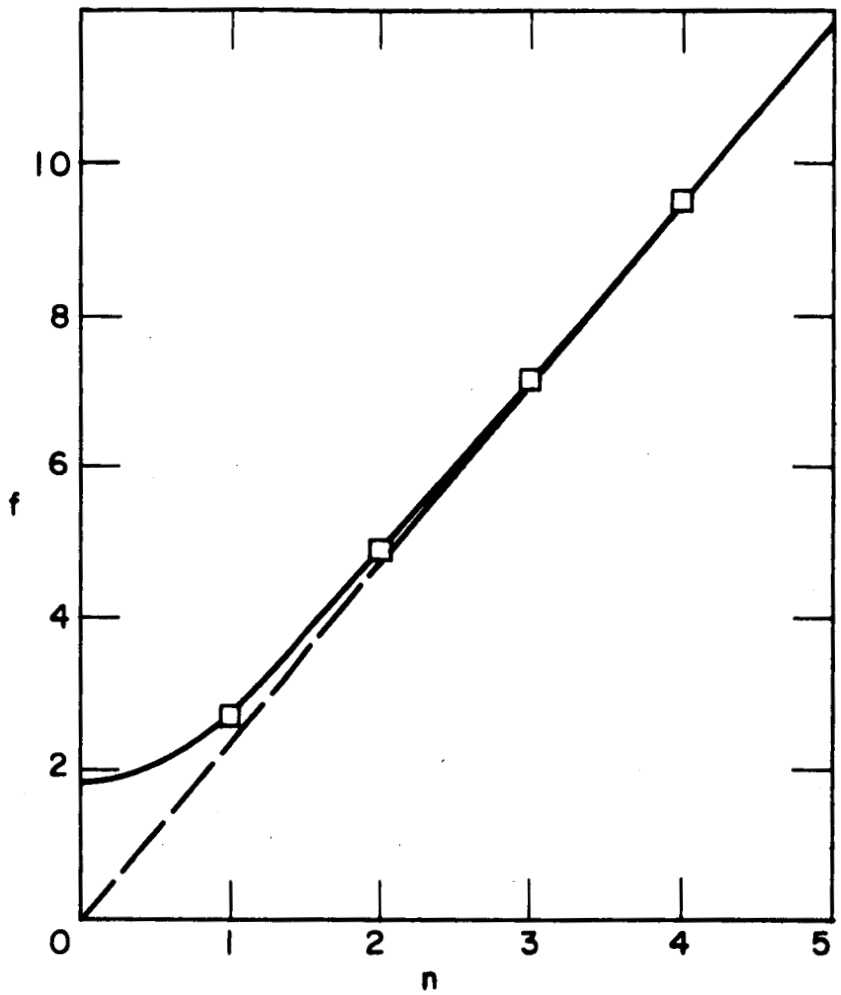

Figure 12. Experimental eigenfrequency vs. mode number for zero applied voltage. The deviation from a straight line is caused by the effect of the support strings on the elastic structure (spring).

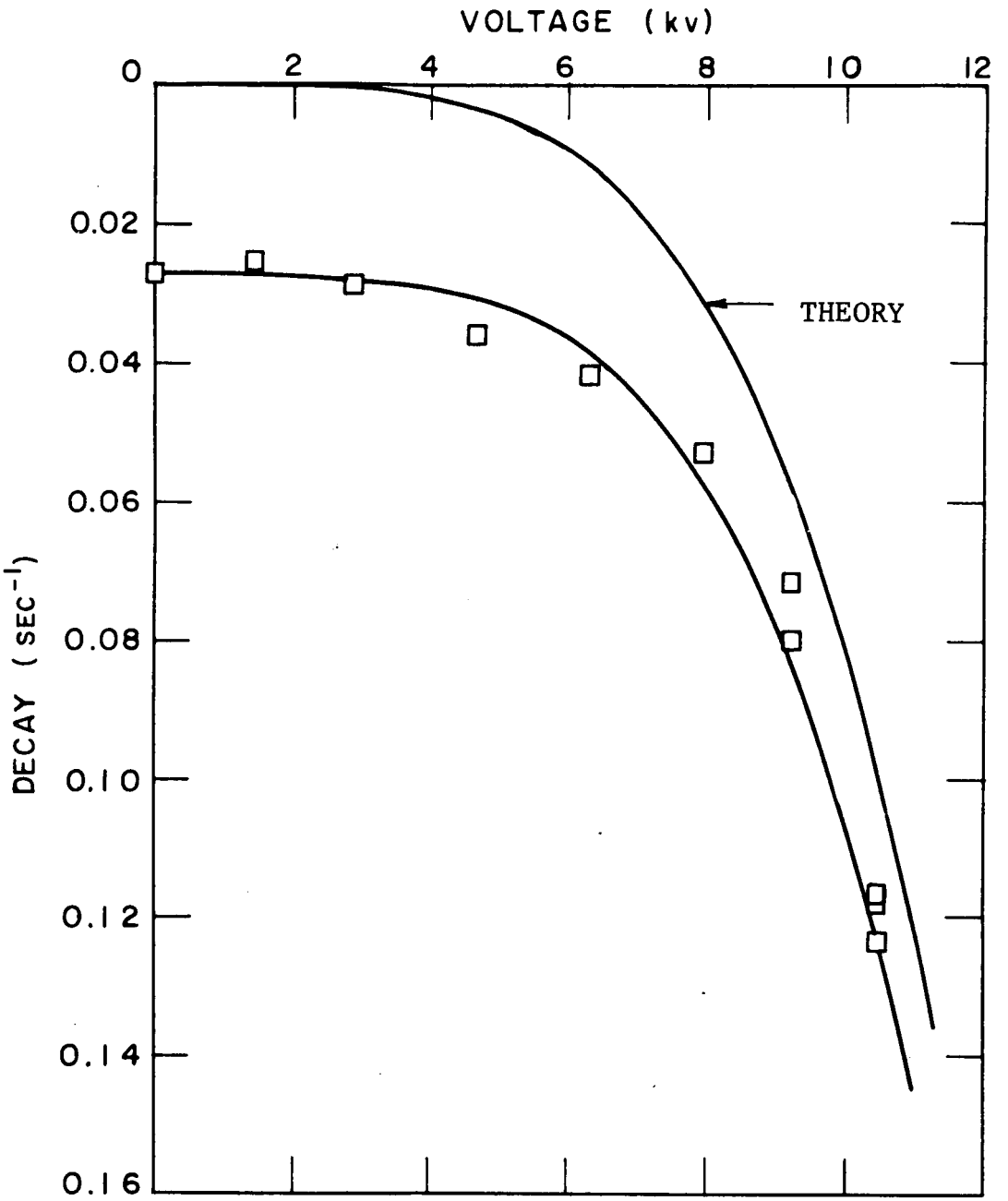

Figure 13. Imaginary part of eigenfrequency vs. applied voltage for the lowest four modes. The lower solid curve is the theoretical curve corrected for the mechanical damping at zero voltage. The instability of the third mode is apparent in (c).

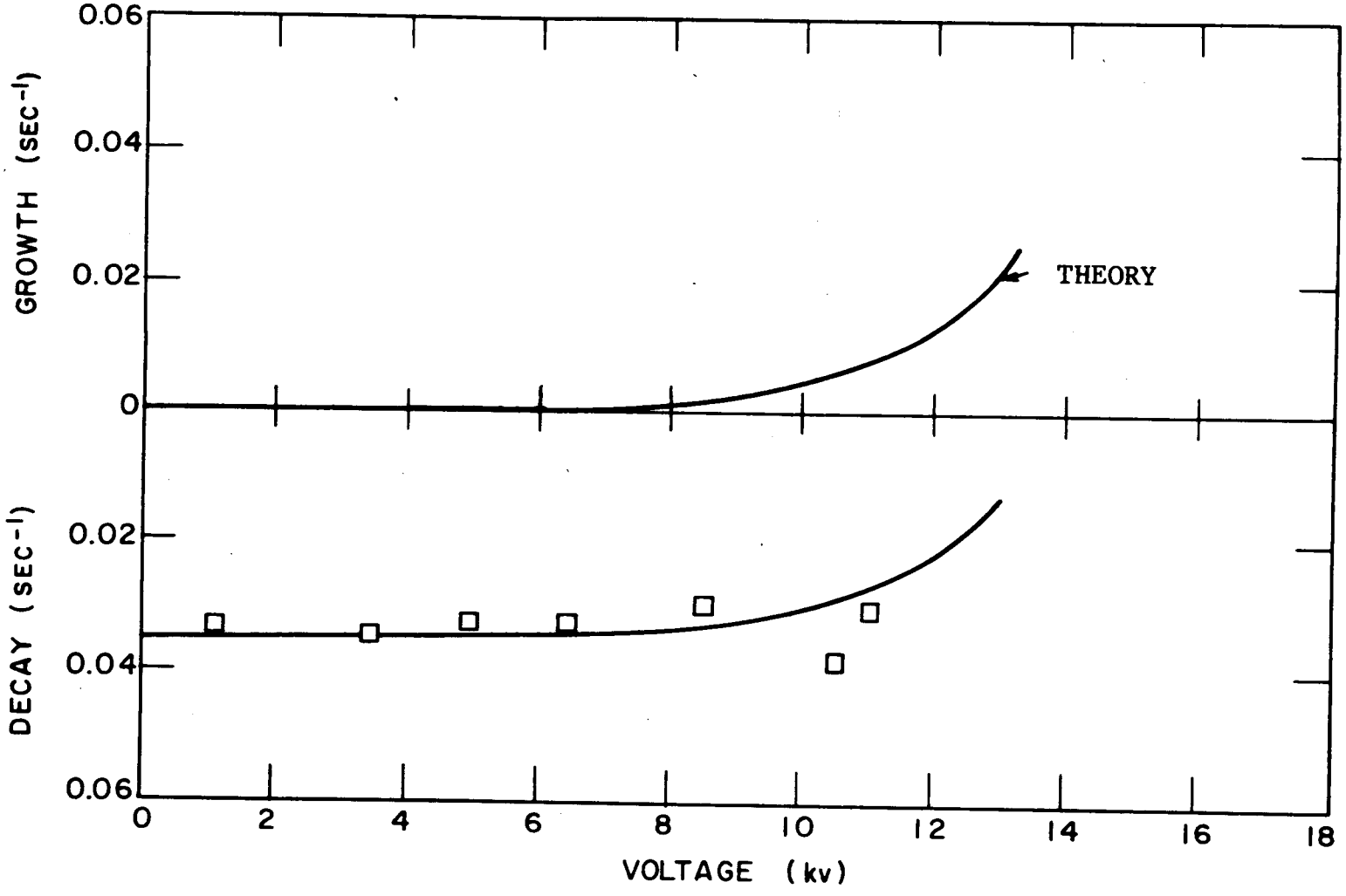

FIGURE 13 b DECAY VS VOLTAGE, MODE #2

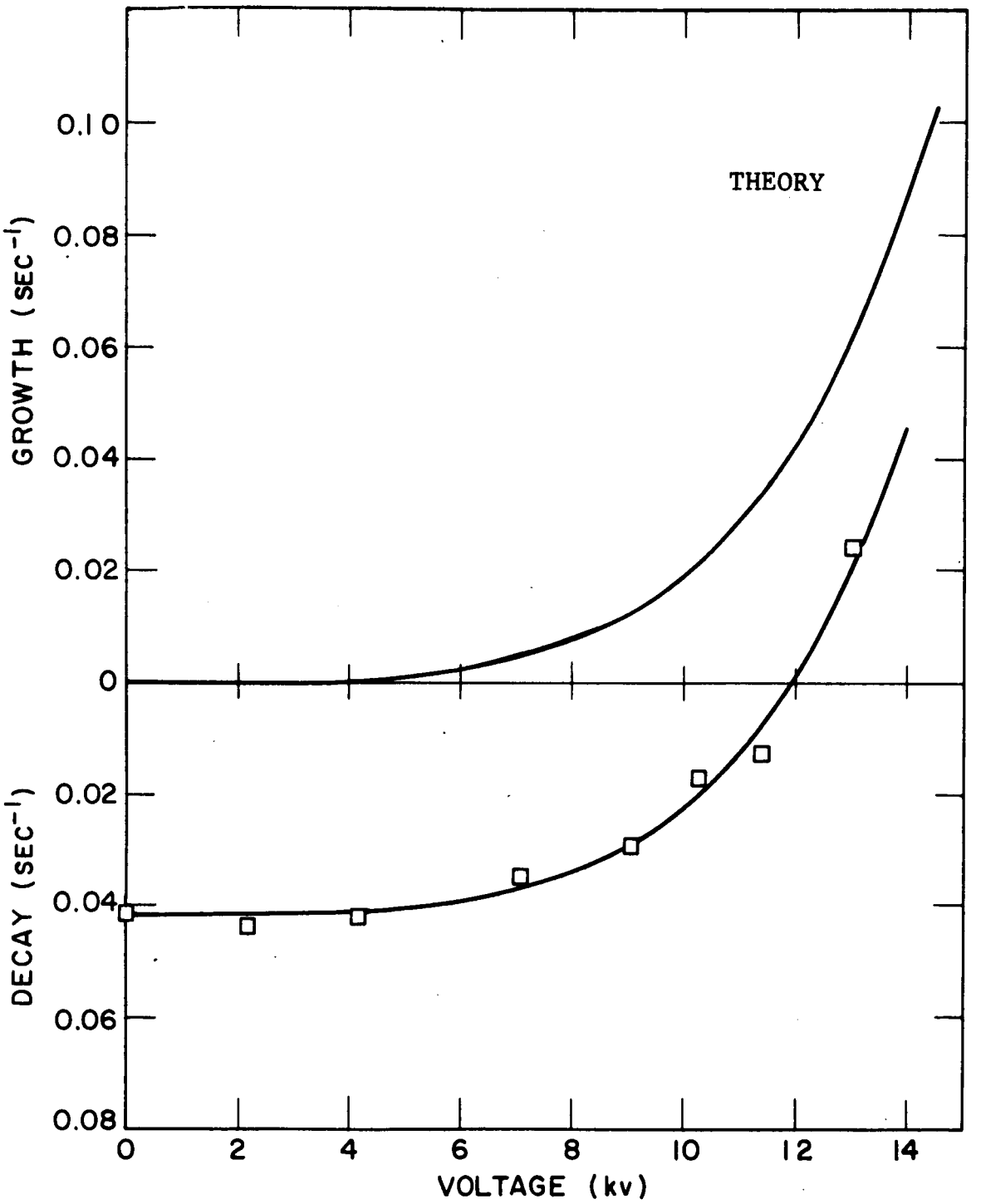

FIGURE 13 c DECAY VS VOLTAGE, MODE #3

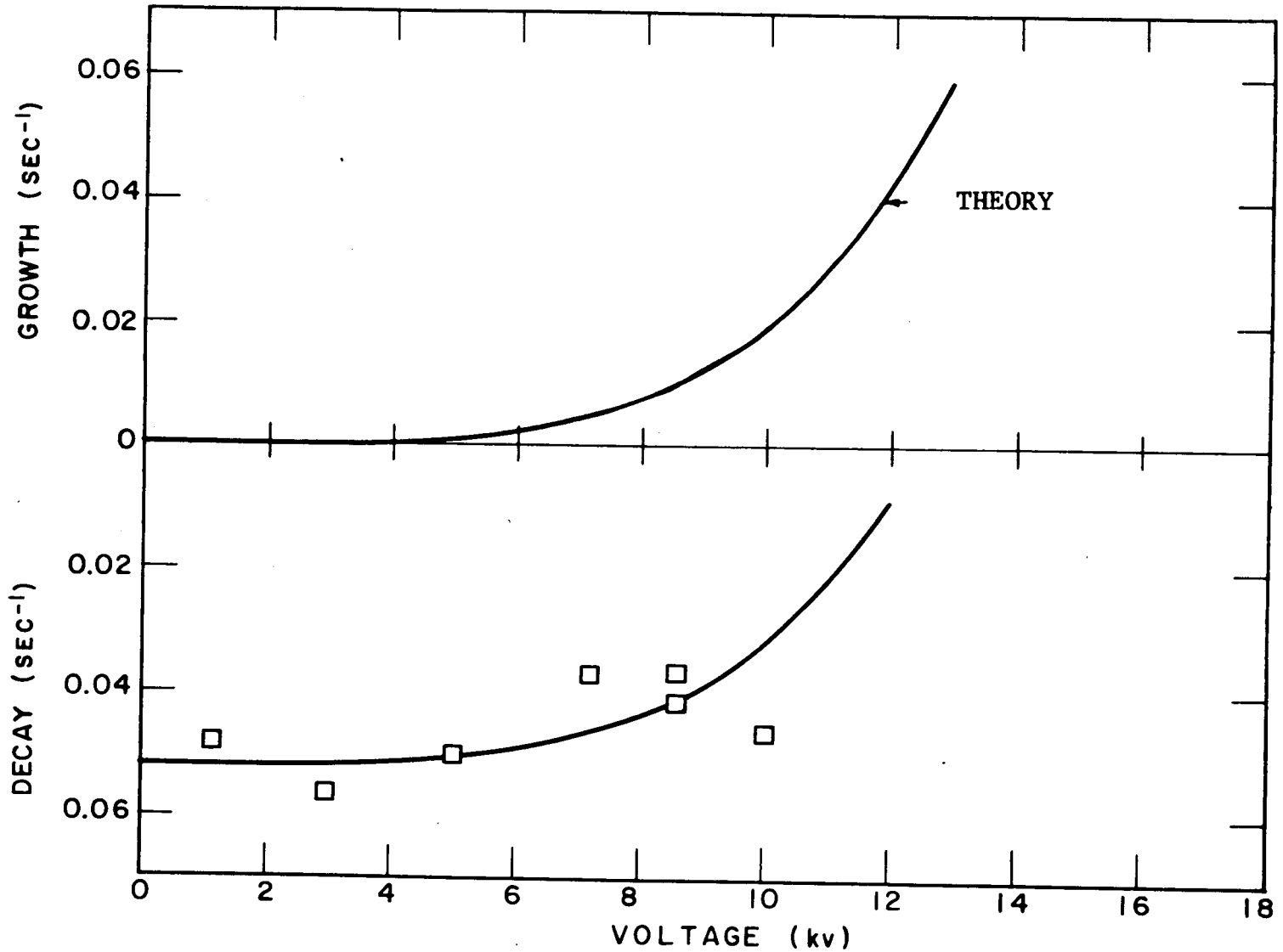

FIGURE 13 d DECAY VS. VOLTAGE, MODE #4

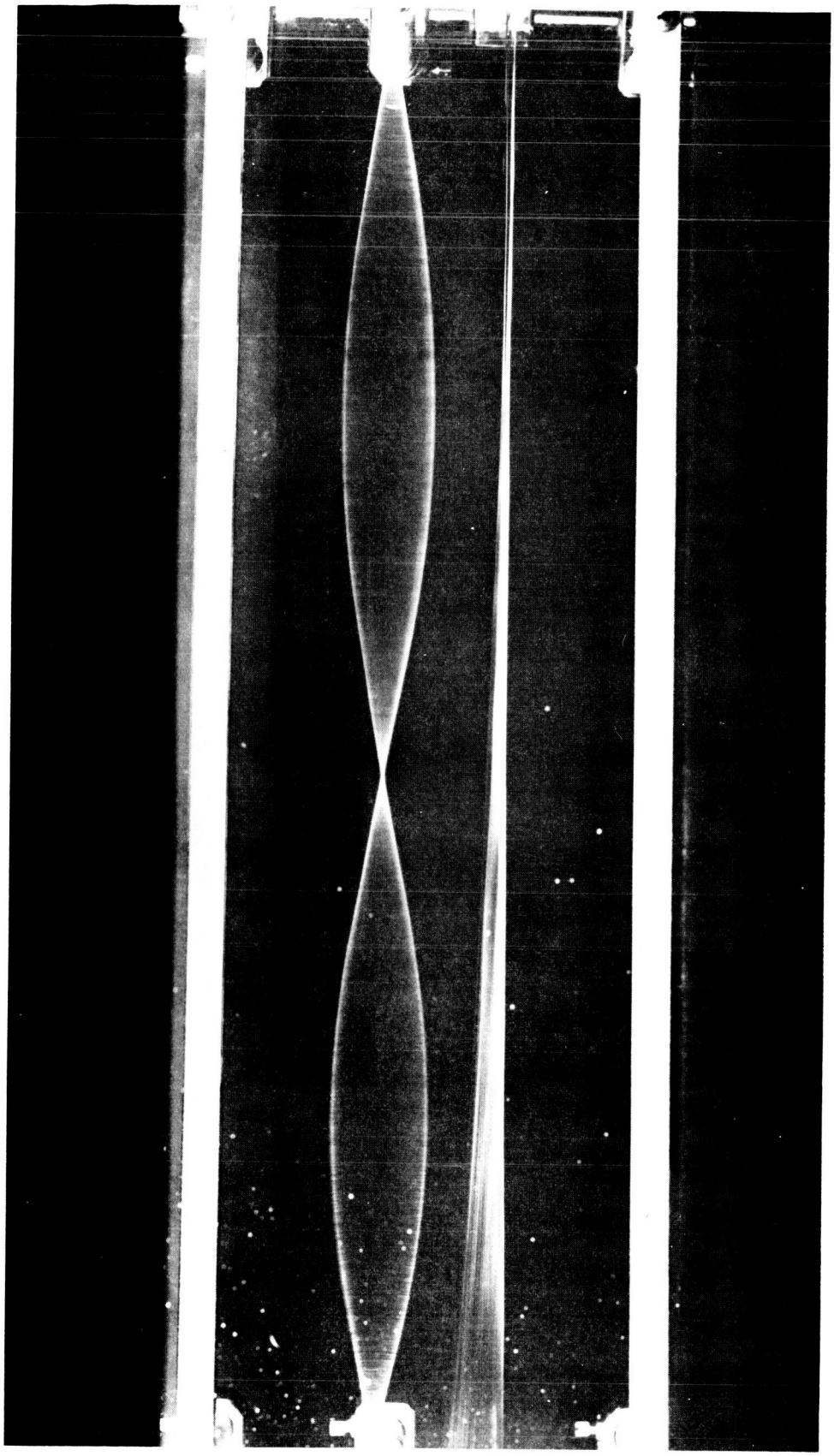

Figure 14. Time exposure for one period of oscillation during build-up of electric field coupled streaming overstability. Spring (left) and jet (right) are resonating at the second eigenfrequency.

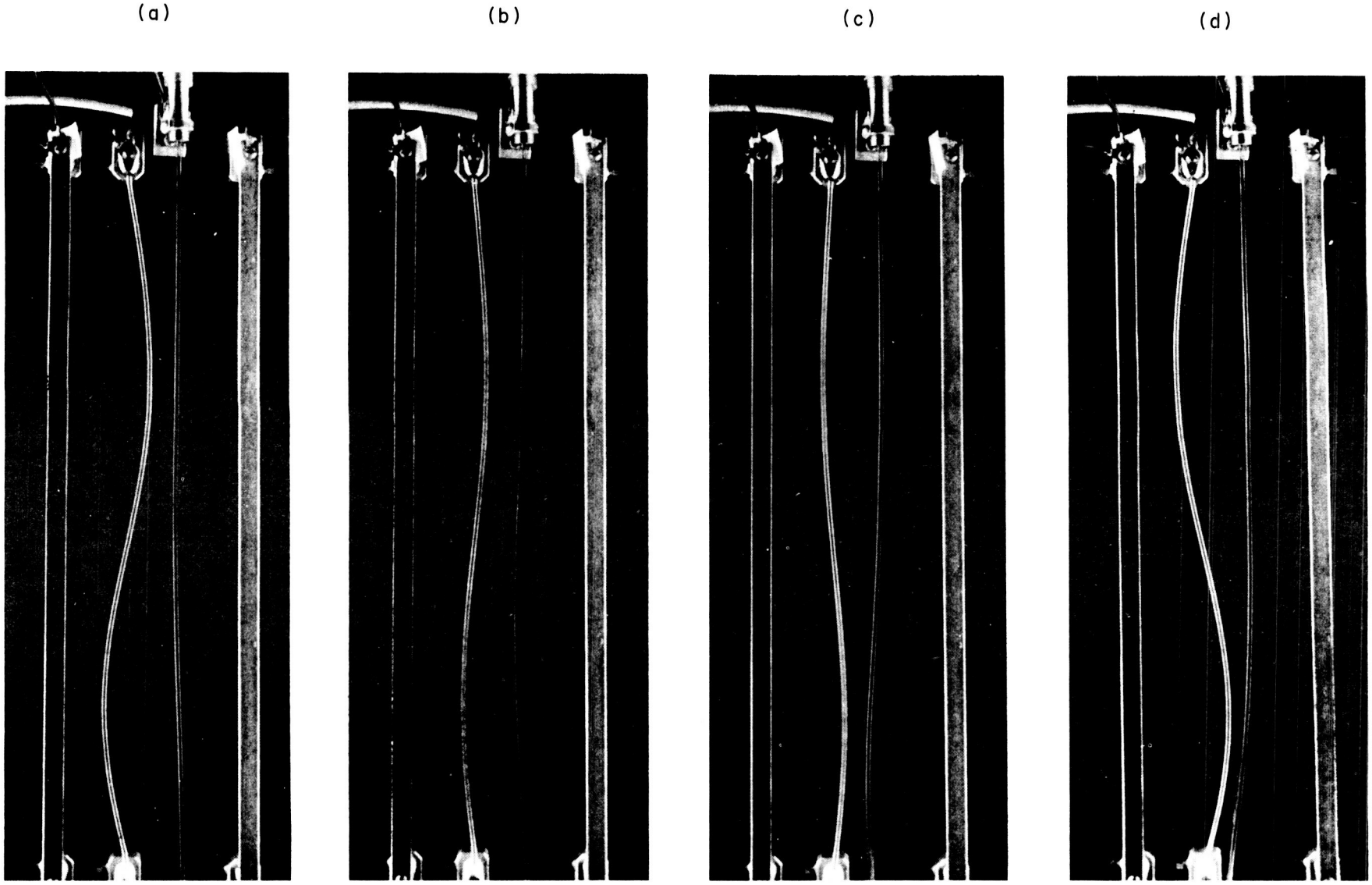

Figure 15. High speed photographs of the streaming overstability in Figure 14. The time interval between exposures is about 60° in phase. The frequency of oscillation is about 7 cps.

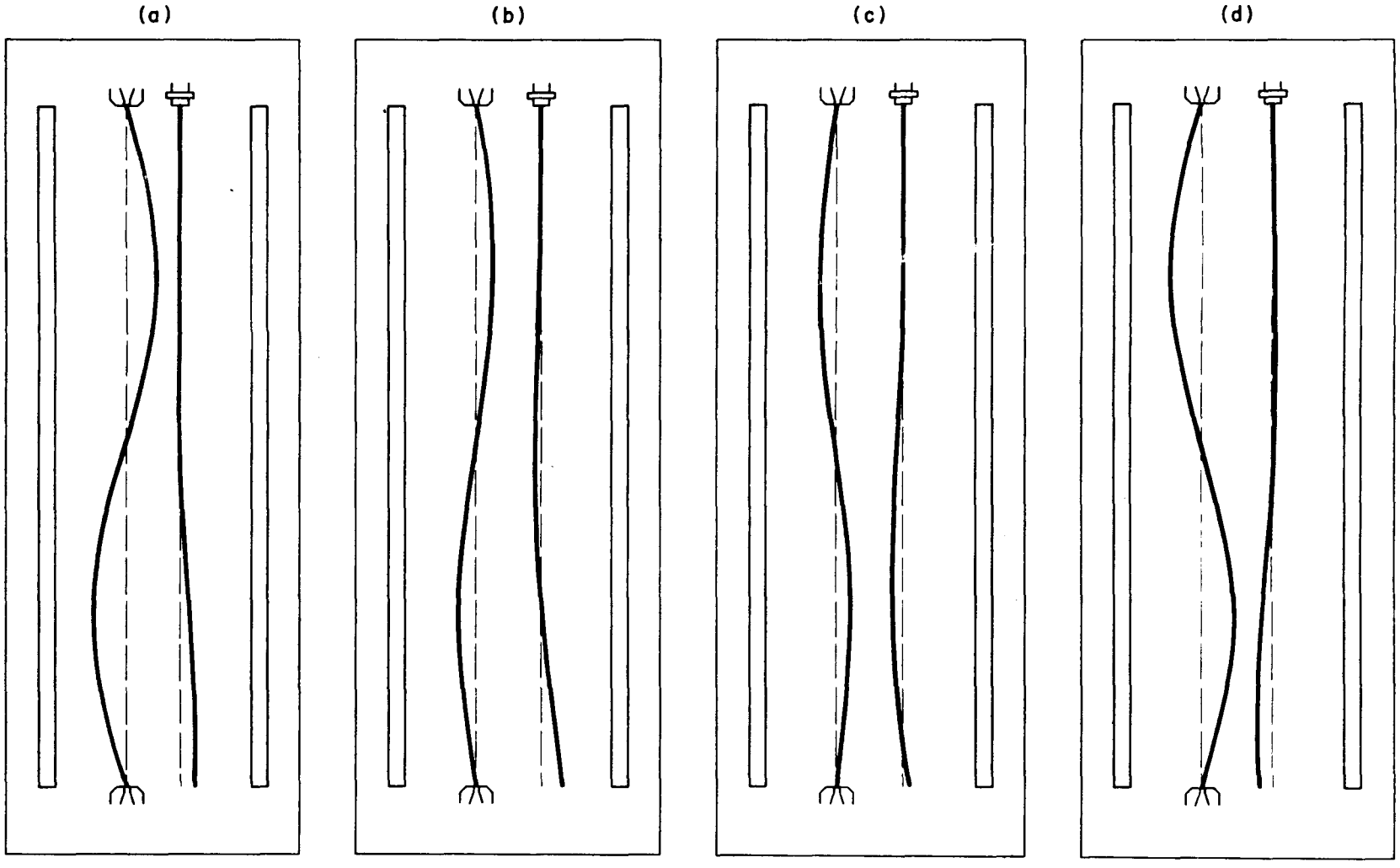

Figure 16. Theoretical eigenfunctions for the experimental conditions of Figure 15.